10.1098/rspa.2001.0950

THE ROYAL SOCIETY

Lamb wave propagation in inhomogeneous elastic waveguides

By Vincent Pagneux[1] and Agnès Maurel[2]

[1]*Laboratoire d'Acoustique de l'Université du Maine, UMR CNRS 6613, Av. Olivier Messiaen, 72085 Le Mans Cedex 9, France*

[2]*Laboratoire Ondes et Acoustique, UMR CNRS 7587, Ecole Supérieure de Physique et de Chimie Industrielles, 10 rue Vauquelin, 75005 Paris, France*

Received 9 April 2001; revised 27 July 2001 and 23 November 2001; accepted 30 November 2001

The problem of Lamb wave propagation in an axially multi-layered waveguide is treated by a multi-modal approach. A general formalism is proposed that avoids the numerical divergence due to evanescent modes and that is based on an impedance matrix. To describe the fields, we choose a 4-vector composed of the displacements and the horizontal stresses. Due to symmetry properties of the right- and left-going modes, this 4-vector can be split into two 2-vectors described by only two sets of modal components. Moreover, the modal 2-vectors have a biorthogonality relation that allows us to express the fields continuity at the interface between two media in a simple manner. Formally, this approach permits us to extend the multi-modal formalism from fluidic to elastic waveguides. In this context, the impedance matrix is defined as the linear operator that links the two sets of modal components. As in the fluidic case, the impedance matrix has the advantage of avoiding numerical divergence, and can be used to obtain the reflection and transmission matrices, as well as the wave fields. The technique is validated in the case of two semi-infinite elastic plates bounded along their lateral faces (succession of two media) and is also applied to a thick bonding (succession of three media) and to a periodic waveguide (succession of multiple media).

Keywords: elastic waveguide; impedance matrix; Lamb modes; multi-modal method; layered structure; scattering

1. Introduction

A modal approach is generally well adapted to treat a problem of guided waves because transverse modes naturally appear and it permits the reduction of the problem to an ordinary differential equation that governs the modal components, and that results from the projection onto the modal basis. For instance, fluidic waveguides can be easily treated in this manner, and the obtained modes take a very simple form (Morse & Ingard 1952). For elastic waveguides, in the case of in-plane motion, the transverse modes are the so-called Lamb modes, which are much more delicate to use (Auld 1973, p. 198). Consequently, compared with fluidic waveguides, relatively

few studies in elastic waveguides have been performed using a multi-modal approach. In particular, there is no general multi-modal method to treat axially multi-layered waveguides (segmented along the length). Concerning two semi-infinite elastic plates bounded along their lateral faces, Scandrett & Vasudevan (1991) succeeded in calculating transmission coefficients using a multi-modal approach. Predoi & Rousseau (2000) used the same kind of technique to solve the case of welded plates (soldered joint). Galanenko (1998) proposed a coupled-mode theory for range-dependent elastic waveguides. Very recently, Folguera & Harris (1999) solved the problem of an elastic waveguide with slowly varying thickness, and applied their technique to the study of coupled surface waves. We can also mention the works of Gregory & Gladwell (1983) concerning the case of reflection from fixed or free edges.

Certainly, the main difficulty is the lack of a general formalism that would be applicable to any layered waveguide, and could permit us to avoid the numerical divergence due to the evanescent modes. One could try to neglect these evanescent modes; however, they are necessary to obtain a consistent multi-modal method. Moreover, these evanescent modes are physically important because they contribute to the near field of any inhomogeneity in the waveguide.

This divergence difficulty also exists in fluidic case, but it can be circumvented by introducing the impedance matrix Z, which is the linear operator linking together pressure and velocity in the modal representation (Pagneux *et al*. 1996), and which is the generalization of the classical scalar impedance to multi-modal propagation. This impedance operator is the counterpart to the so-called Dirichlet-to-Neumann operator in applied mathematics, and allows us to settle the boundary condition imposed by the physical radiation condition. Once a radiation condition is given at the outlet of the waveguide, this impedance matrix can be calculated everywhere, either by integrating a matricial Riccati equation in the case of continuously inhomogeneous guide (Pagneux *et al*. 1996), or by directly using algebraic relations in the case of a discontinuously inhomogeneous guide. When dealing with evanescent modes, the matrix Z has the important advantage of being divergence free. It is then used to obtain, without numerical divergence, either the fields (e.g. pressure and velocity) or the reflection and transmission matrices of the waveguide. A heuristic explanation that helps us to understand the non-divergence of the impedance matrix is to recall that the impedance represents the ratio of the pressure to the velocity, and that this ratio does not diverge when pressure and velocity diverge with the same logarithmic decrement, which is the case for an evanescent mode.

In this paper, we introduce an equivalent of the impedance matrix for elastic propagation in waveguides. First, assuming the completeness of Lamb modes, the four fields, composed of the two components (u and v) of the displacements and the two components (s and t) of the axial stress, are projected on these modes. In this context, we assemble the four fields into two pairs of vectors $\boldsymbol{X} = (u, t)^{\mathrm{T}}$ and $\boldsymbol{Y} = (-s, v)^{\mathrm{T}}$ related to vectors $\boldsymbol{a}$ and $\boldsymbol{b}$ as $\boldsymbol{X} = \sum_n a_n \boldsymbol{X}_n$ and $\boldsymbol{Y} = \sum_n b_n \boldsymbol{Y}_n$. This formalism has two advantages. First, our vectorial problem now mimics the scalar problem of fluidic waveguides, since the two unknown vectors $\boldsymbol{X}$ and $\boldsymbol{Y}$ are expressed in terms of two component vectors $\boldsymbol{a}$ and $\boldsymbol{b}$ in the same manner as for the two scalars (pressure and longitudinal velocity) in fluidic waveguide. The second advantage is that the biorthogonal relation due to Fraser (1976) makes the set of vectors $\boldsymbol{X}_n$ and $\boldsymbol{Y}_n$ to form a biorthogonal basis; thus continuity relations involving the two components of vector $\boldsymbol{X}$ (respectively, $\boldsymbol{Y}$) are easily projected on this basis and yield continuity

Author: leading ^{t} changed to trailing $^{\mathrm{T}}$ (matrix transpose) – OK?

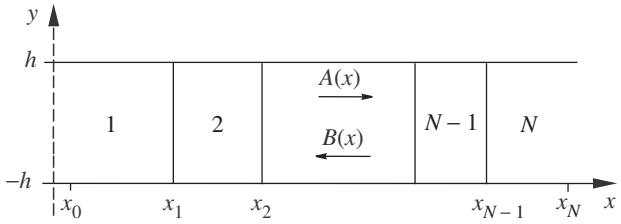

Figure 1. Geometry of the Lamb wave problem for a succession of media.

relations for the components a_n (respectively, b_n). The impedance matrix $\boldsymbol{Z}$ is defined as the linear operator that links $\boldsymbol{b}$ to $\boldsymbol{a}$ by $\boldsymbol{b} = \boldsymbol{Z}\boldsymbol{a}$. By construction, $\boldsymbol{Z}$ is equal to the identity matrix $\boldsymbol{I}$ when there are only right-going waves and equal to $-\boldsymbol{I}$ when there are only left-going waves. This impedance matrix can be calculated everywhere from the radiation condition at the outlet of the elastic waveguide, and it induces no numerical divergence. Thereafter, the reflection and transmission coefficients, as well as the entire field, can be determined.

The paper's outline is as follow. In § 2, the Lamb mode problem is presented and the modal decomposition is performed; this leads to the definition of vectors $\boldsymbol{X}$, $\boldsymbol{Y}$ 'associated' by the biorthogonality relation. The impedance matrix is introduced in § 3 as the linear operator that links $\boldsymbol{a}$ and $\boldsymbol{b}$; the evolution of $\boldsymbol{Z}$ in a single medium and at a junction is presented (discussion of the divergence-free property of $\boldsymbol{Z}$ is given in the appendix). The expressions of the transmission and reflection matrices are derived in § 4 for a succession of media, i.e. for a axially layered waveguide. In § 5, calculations are presented that allow us to obtain the displacement and stress fields in the presence of a source. Then § 6 presents the derivation of the energy-flux ratio of the reflected and transmitted waves. Finally, results are presented in § 7. First, the method is briefly validated in the case (already studied by Scandrett & Vasudevan (1991)) of two semi-infinite elastic plates bounded along their lateral faces. The cases of a thick bonding and of a periodic medium are then studied.

2. Position of the problem

(*a*) *Equations*

The Lamb wave problem consists of looking for a solution of the elasticity equation in the waveguide defined by $-h \leqslant y \leqslant h$ with free boundaries, and for which displacements are in the (x, y)-plane (see figure 1). The monochromatic time dependence, with pulsation ω, is $\mathrm{e}^{-\mathrm{i}\omega\tau}$ and will be omitted in the following. The equation of motion is

$$-\rho\omega^2\boldsymbol{w} = \operatorname{div}\sigma, \tag{2.1}$$

where ρ is the density, $\boldsymbol{w} =^t (u, v)$ is the vector of displacements and σ is the stress tensor defined by

$$\sigma = \begin{pmatrix} s & t \\ t & r \end{pmatrix}, \tag{2.2}$$

with

$$s = \lambda \partial_y v + (\lambda + 2\mu)\partial_x u, \tag{2.3a}$$

$$t = \mu(\partial_y u + \partial_x v), \tag{2.3b}$$

$$r = (\lambda + 2\mu)\partial_y v + \lambda \partial_x u. \tag{2.3c}$$

where λ, μ are Lamé's constants.

The faces $y = \pm h$ are free of traction, corresponding to boundary conditions

$$t(x, \pm h) = r(x, \pm h) = 0. \tag{2.4}$$

We are interested in the propagation of a Lamb wave through a succession of media (figure 1). The boundary condition at the junction $x = x_1$ between two media corresponds to the stress and displacement continuities, i.e. u, v, s, t continuous at $x = x_1$.

(*b*) *Modal decomposition*

For a given homogeneous waveguide (independent of x), the Lamb mode can be found by separating variables x and y in the form

$$\begin{pmatrix} u(x,y) \\ v(x,y) \\ s(x,y) \\ t(x,y) \end{pmatrix} = \begin{pmatrix} \hat{u}(y) \\ \hat{v}(y) \\ \hat{s}(y) \\ \hat{t}(y) \end{pmatrix} \mathrm{e}^{\mathrm{i}kx}. \tag{2.5}$$

This leads to an eigenvalue problem for k whose solutions form a discrete spectrum (Achenbach 1987; Auld 1973; Miklowitz 1978). The spectrum can be split in two parts. The right-going waves correspond to eigenvalues with strictly positive imaginary parts or positive group velocity for real eigenvalues. The left-going waves correspond to eigenvalues with strictly negative imaginary parts or negative group velocity for real eigenvalues. We choose to index by integer n the eigenvalues corresponding to right-going waves, and we call them k_n ($\mathrm{Im}(k_n) > 0$ or $v_\mathrm{g} = (\mathrm{d}k_n/\mathrm{d}\omega)^{-1} > 0$ when k_n is real). The eigenvalues k_n are sorted in ascending order of their imaginary part and descending order of their real part. As a consequence of the central symmetry of the spectrum $k \to -k$ (see equation (A 1)), if k_n is a right-going wave, $-k_n$ is an eigenvalue and it corresponds to left-going waves ($\mathrm{Im}(k_n) < 0$ or negative group velocity $v_\mathrm{g} = (\mathrm{d}k_n/\mathrm{d}\omega)^{-1} < 0$ when k_n is real). A method of obtaining the k_n values can be found in Pagneux & Maurel (2001). The so-called Lamb modes are the associated eigenfunctions $(U_n(y), V_n(y), S_n(y), T_n(y))^\mathrm{T}$, corresponding to k_n for a right-going wave, and $(\tilde{U}_n(y), \tilde{V}_n(y), \tilde{S}_n(y), \tilde{T}_n(y))^\mathrm{T}$, corresponding to $-k_n$ for a left-going wave. Note that eigenvalues and eigenfunctions implicitly depend on the parameters of the medium λ, μ and ρ.

For an inhomogeneous waveguide whose parameters λ, μ and ρ depend on x, if we assume the completeness of the eigenfunctions (Kirrmann 1995), the fields u, v, s and t can be decomposed on the Lamb modes at each x,

$$\begin{pmatrix} u(x,y) \\ v(x,y) \\ s(x,y) \\ t(x,y) \end{pmatrix} = \sum_{n\in\mathbb{N}} A_n(x) \begin{pmatrix} U_n(y) \\ V_n(y) \\ S_n(y) \\ T_n(y) \end{pmatrix} + \sum_{n\in\mathbb{N}} B_n(x) \begin{pmatrix} \tilde{U}_n(y) \\ \tilde{V}_n(y) \\ \tilde{S}_n(y) \\ \tilde{T}_n(y) \end{pmatrix}, \tag{2.6}$$

and for a locally homogeneous portion of the waveguide, the amplitude $A_n(x)$ (respectively, $B_n(x)$) behaves as $\exp(\mathrm{i}k_n x)$ (respectively, $\exp(-\mathrm{i}k_n x)$).

The symmetry properties of the Lamb modes impose $\tilde{U}_n = -U_n$, $\tilde{V}_n = V_n$, $\tilde{S}_n = S_n$ and $\tilde{T}_n = -T_n$ (see Appendix A for the example of symmetric modes). Defining the coefficients $a_n(x)$, $b_n(x)$ as

$$a_n(x) = A_n(x) - B_n(x), \qquad b_n(x) = A_n(x) + B_n(x), \tag{2.7}$$

we obtain

$$\begin{pmatrix} u(x,y) \\ v(x,y) \\ s(x,y) \\ t(x,y) \end{pmatrix} = \sum_{n\in\mathbb{N}} \begin{pmatrix} a_n(x)U_n(y) \\ b_n(x)V_n(y) \\ b_n(x)S_n(y) \\ a_n(x)T_n(y) \end{pmatrix}. \tag{2.8}$$

Then the biorthogonality relation (cf. Fraser (1976); see also Murphy & Li (1994) for a generalization)

$$\int_{-h}^{h} (-U_n(y)S_m(y) + T_n(y)V_m(y))\,\mathrm{d}y = J_n\delta_{nm}$$

allows us to write the fields as

$$\boldsymbol{X} = \sum_{n\in\mathbb{N}} a_n(x)\boldsymbol{X_n}(y), \quad \boldsymbol{Y} = \sum_{n\in\mathbb{N}} b_n(x)\boldsymbol{Y_n}(y) \quad \text{and} \quad (\boldsymbol{X_m} \mid \boldsymbol{Y_n}) = J_n\delta_{mn}, \tag{2.9}$$

with

$$\boldsymbol{X} = \begin{pmatrix} u(x,y) \\ t(x,y) \end{pmatrix}, \quad \boldsymbol{Y} = \begin{pmatrix} -s(x,y) \\ v(x,y) \end{pmatrix}, \quad \boldsymbol{X_n}(y) = \begin{pmatrix} U_n(y) \\ T_n(y) \end{pmatrix}, \quad \boldsymbol{Y_n}(y) = \begin{pmatrix} -S_n(y) \\ V_n(y) \end{pmatrix},$$

and the scalar product defined by

$$(\boldsymbol{X} \mid \boldsymbol{Y}) = \int_{-h}^{h} (-us + tv)\,\mathrm{d}y.$$

The analytical expression of J_n is given in Appendix B for symmetric modes. Equation (2.9) is important in our formalism, because the two series of components a_n and b_n can be isolated simply by taking the scalar product of $\boldsymbol{X}$ (respectively, $\boldsymbol{Y}$) with $\boldsymbol{Y_n}$ (respectively, $\boldsymbol{X_n}$), since $(\boldsymbol{X} \mid \boldsymbol{Y_n}) = J_n a_n$ and $(\boldsymbol{Y} \mid \boldsymbol{X_n}) = J_n b_n$.

3. Impedance matrix

Owing to the formalism developed in the preceding section (equation (2.9)), the problem of the propagation of Lamb waves resembles the problem of scalar wave propagation. This means that a transfer matrix can be obtained easily for a succession of N media by multiplying successive transfer matrices of junction and single media. Note that the way of expressing the fields in (2.9) associated with the biorthogonality relation is crucial to easily treat the transfer matrix of a junction, which is obtained by using the continuity of $\boldsymbol{X}$ and $\boldsymbol{Y}$. Nevertheless, the transfer matrix method is numerically unstable due to exponentially diverging terms associated with evanescent modes. Therefore, one is led to the introduction of the impedance matrix that

circumvents this numerical instability (note that it could also be possible to use a reflection matrix).

The impedance matrix $\mathsf{Z}(x)$ is defined as the linear operator that links together vectors $\boldsymbol{a}(x)$ and $\boldsymbol{b}(x)$ at a given x position,

$$\boldsymbol{b}(x) = \mathsf{Z}(x)\boldsymbol{a}(x). \tag{3.1}$$

In this section, we show that $\mathsf{Z}(x)$ can be calculated in the domain formed by the succession of the two media separated by a $x = x_1$ junction and, by extension, to a succession of N media.

(*a*) *Propagation relation for the impedance matrix in a single medium*

In a given medium (ρ, λ and μ constant), the impedance matrix $\mathsf{Z}(x')$ can be calculated by linking together $\mathsf{Z}(x')$ and $\mathsf{Z}(x)$ (which is known). As $\boldsymbol{A}$ refers to a right-going wave and $\boldsymbol{B}$ to a left-going wave, we have

$$A_n(x') = A_n(x)\exp[\mathrm{i}k_n(x'-x)], \qquad B_n(x') = B_n(x)\exp[-\mathrm{i}k_n(x'-x)], \tag{3.2}$$

as was already noted in § 2 *b*. It follows that $\boldsymbol{a}(x')$ and $\boldsymbol{b}(x')$ can be deduced from $\boldsymbol{a}(x)$ and $\boldsymbol{b}(x)$ using (2.7) and (3.2),

$$\begin{pmatrix}\boldsymbol{a}(x')\\ \boldsymbol{b}(x')\end{pmatrix} = \begin{pmatrix}\mathsf{C}(x'-x) & \mathrm{i}\mathsf{S}(x'-x)\\ \mathrm{i}\mathsf{S}(x'-x) & \mathsf{C}(x'-x)\end{pmatrix}\begin{pmatrix}\boldsymbol{a}(x)\\ \boldsymbol{b}(x)\end{pmatrix}, \tag{3.3}$$

where $\mathsf{C}(x'-x)$ is the diagonal matrix with $\cos[k_n(x'-x)]$ elements and $\mathsf{S}(x'-x)$ is the diagonal matrix with $\sin[k_n(x'-x)]$ elements. The transfer matrix that appears in equation (3.3) has the disadvantage of having exponentially diverging terms, since the wavenumbers k_n are complex for evanescent modes, and $\mathrm{Im}(k_n) \to \infty$ when $n \to \infty$. Thus the transfer matrix is numerically unstable, in contrast to the impedance matrix expression given below. The relation between $\mathsf{Z}(x')$ and $\mathsf{Z}(x)$ is deduced from (3.3),

Word added – OK?

$$\mathsf{Z}(x') = -\mathrm{i}\mathsf{H}^{-1}(x'-x) + \mathsf{S}^{-1}(x'-x)(\mathsf{Z}(x) - \mathrm{i}\mathsf{H}^{-1}(x'-x))^{-1}\mathsf{S}^{-1}(x'-x), \tag{3.4}$$

where $\mathsf{S}^{-1}(x'-x)$ is the diagonal matrix with $1/\sin k_n(x'-x)$ elements and $\mathsf{H}^{-1}(x'-x)$ is the diagonal matrix with $1/\tan[k_n(x'-x)]$ elements.

By construction, $\mathsf{Z}(x)$ does not diverge for evanescent modes. However, care has to be taken such that $\mathsf{Z}(x')$ is calculated starting from $\mathsf{Z}(x)$ with $x' < x$. This point and the derivation of (3.4) are discussed in Appendix C.

(*b*) *Transfer relation for the impedance matrix at a junction*

In the previous section, we have shown that $\mathsf{Z}(x)$ can be propagated in a given medium. In order to propagate $\mathsf{Z}(x)$ in a succession of media, we now want to propagate $\mathsf{Z}(x)$ from one medium to another through the $x = x_1$ junction or, in other words, link together the impedance matrix $\mathsf{Z}(x_1^+)$ and $\mathsf{Z}(x_1^-)$ (see figure 1). The stress and displacement continuities at the junction $x = x_1$ are written as

$$\sum_{n\in\mathbb{N}} a_n(x_1^-)X_n^-(y) = \sum_{n\in\mathbb{N}} a_n(x_1^+)X_n^+(y), \tag{3.5 a}$$

$$\sum_{n\in\mathbb{N}} b_n(x_1^-)Y_n^-(y) = \sum_{n\in\mathbb{N}} b_n(x_1^+)Y_n^+(y), \tag{3.5 b}$$

where superscript $-$ (respectively, $+$) on the transverse modes X_n and Y_n signifies that these modes correspond to the medium at $x = x_1^-$ (respectively, $x = x_1^+$). Taking the scalar product of (3.5 *a*) by Y_m^+ and of (3.5 *b*) by X_m^-, and using the biorthogonality relation, we obtain

$$\boldsymbol{b}(x_1^-) = \mathsf{F}\boldsymbol{b}(x_1^+), \tag{3.6 a}$$

$$\boldsymbol{a}(x_1^+) = \mathsf{G}\boldsymbol{a}(x_1^-), \tag{3.6 b}$$

with the matrices F and G defined by

$$\left.\begin{aligned} \mathsf{F}_{mn} &= (J_n^-)^{-1}(X_m^- \mid Y_n^+), \\ \mathsf{G}_{mn} &= (J_n^+)^{-1}(X_n^- \mid Y_m^+). \end{aligned}\right\} \tag{3.7}$$

The analytical expressions of F and G are given in Appendix D for symmetric modes. Using (3.1) in (3.6), the relation between $\mathsf{Z}(x_1^-)$ and $\mathsf{Z}(x_1^+)$ is found,

$$\mathsf{Z}(x_1^-) = \mathsf{F}\mathsf{Z}(x_1^+)\mathsf{G}. \tag{3.8}$$

In this section, we have established the relations (3.4) and (3.8) that allow us to calculate $\mathsf{Z}(x)$ in the whole space (formed of multiple media) independently of the nature of the source. Consequently, the calculation for $\mathsf{Z}(x)$ can be performed by starting from the radiation condition at the end of the waveguide, and by calculating $\mathsf{Z}(x)$ towards the waveguide inlet. Note that, more generally, the impedance matrix could be used in a finite-element method to ensure an exact radiation condition at the extremities of the waveguide (Givoli 1992).

4. Reflection and transmission matrices

In order to solve scattering problems in the type of considered waveguides (figure 1), we are led to introduce the reflection and transmission matrices in this section. We define the reflection matrix $\mathsf{R}(x)$ as the linear operator that links the right- and the left-going waves at a given x position,

$$\boldsymbol{B}(x) = \mathsf{R}(x)\boldsymbol{A}(x). \tag{4.1}$$

On the other hand, it is also possible to define the transmission matrix that relates the right-going wave between x and x',

$$\boldsymbol{A}(x') = \mathsf{T}(x', x)\boldsymbol{A}(x). \tag{4.2}$$

The issue of expressing R is quite straightforward when the impedance matrix is already known, since the following relation is obtained from equations (2.7), (3.1) and (4.1),

$$\mathsf{R}(x) = [\mathsf{Z}(x) - \mathsf{I}][\mathsf{Z}(x) + \mathsf{I}]^{-1}, \tag{4.3}$$

where I is the identity matrix. The calculation of T is not always as straightforward, and is given for the considered case in the next sections.

(*a*) *Transmission matrix for a given medium*

An expression for $\mathsf{T}(x', x)$ between two positions x and x' in the same medium (ρ, λ and μ constant) is easily obtained from (3.3),

$$\mathsf{T}(x', x) = \mathsf{E}(x' - x), \tag{4.4}$$

where $\mathsf{E}(x' - x)$ is the diagonal matrix with $\exp[\mathrm{i}k_n(x' - x)]$ on its diagonal. Note that $\mathsf{T}(x', x)$ does not diverge numerically for evanescent modes if $x' \geqslant x$.

(*b*) *Transmission matrices for two media and generalization*

We still consider a junction at $x = x_1$. Using (2.7) and (3.6 *b*), $\mathsf{T}(x_1^+, x_1^-)$ is obtained,

$$\mathsf{T}(x_1^+, x_1^-) = [\mathsf{I} - \mathsf{R}(x_1^+)]^{-1}\mathsf{G}[\mathsf{I} - \mathsf{R}(x_1^-)], \tag{4.5}$$

where R is the reflection matrix and G is defined in equation (3.7). For a succession of N media defined by $N-1$ junctions $x = x_n$ (figure 1), an explicit expression of (4.2) can be obtained using (4.4) and (4.5),

$$\mathsf{T}(x_N, x_0) = \mathsf{E}(x_N - x_{N-1})\mathsf{T}(x_{N-1}^+, x_{N-1}^-)\cdots\mathsf{T}(x_1^+, x_1^-)\mathsf{E}(x_1 - x_0). \tag{4.6}$$

x_N is in the last medium at a distance L_N from the last junction at $x = x_{N-1}$. x_0 is in the first medium at a distance L_0 from the first junction $x = x_1$ (x_0 refers typically to the source location).

5. Determination of the solution in the presence of a source

Once Z, as well as R and T, have been calculated in the whole waveguide, it is possible to take into account the presence of a source. In our formalism, there are two ways to impose a source condition. The first source condition consists of sending a right-going wave from infinity, and this is equivalent to knowing $\boldsymbol{A}(x_0^+)$. The second source condition corresponds to imposing a field value at a given x_0; in order to benefit from the orthogonality condition, this field value has to correspond to a mixed condition, i.e. the knowledge of $\boldsymbol{X}$ or $\boldsymbol{Y}$. In this case, $\boldsymbol{X}(x_0)$ (respectively, $\boldsymbol{Y}(x_0)$) is known, and thus we know $\boldsymbol{A}(x_0)$.

We show here a typical procedure to calculate $\boldsymbol{A}(x)$, $\boldsymbol{B}(x)$ in medium (1) (for $x_0 < x < x_1$) and $\boldsymbol{A}(x_1^+)$ in medium (2). Then this procedure is iterated to calculate the field in a succession of media. It is critical here to take care to propagate evanescent modes towards the direction where they decrease and not back-propagate in a direction where, numerically, a small error would exponentially grow.

Where is medium (1) defined? Likewise, medium (2)

For $x_0 < x < x_1$, $\boldsymbol{A}(x)$ and $\boldsymbol{B}(x)$ can be expressed as a function of $\boldsymbol{A}(x_0^+)$ and $\boldsymbol{B}(x_1^-)$,

$$\begin{pmatrix}\boldsymbol{A}(x)\\ \boldsymbol{B}(x)\end{pmatrix} = \begin{pmatrix}\mathsf{E}(x-x_0) & 0\\ 0 & \mathsf{E}(x_1-x)\end{pmatrix}\begin{pmatrix}\boldsymbol{A}(x_0^+)\\ \boldsymbol{B}(x_1^-)\end{pmatrix}. \tag{5.1}$$

Then, using (4.1) and (4.4), $\boldsymbol{A}(x)$ and $\boldsymbol{B}(x)$ can be expressed as a function of $\boldsymbol{A}(x_0^+)$ only,

$$\begin{pmatrix}\boldsymbol{A}(x)\\ \boldsymbol{B}(x)\end{pmatrix} = \begin{pmatrix}\mathsf{E}(x-x_0) & 0\\ 0 & \mathsf{E}(x_1-x)\mathsf{R}(x_1^-)\mathsf{E}(x_1-x_0)\end{pmatrix}\begin{pmatrix}\boldsymbol{A}(x_0^+)\\ \boldsymbol{A}(x_0^+)\end{pmatrix}, \tag{5.2}$$

with $x_0 < x < x_1$. The displacement and stress fields in medium (1) are then simply calculated using their expressions in (2.6). $\boldsymbol{A}(x_1^+)$ is obtained from $\boldsymbol{A}(x_0^+)$ using (4.2) and (4.5),

$$\boldsymbol{A}(x_1^+) = \mathsf{T}(x_1^+, x_1^-)\mathsf{E}(x_1 - x_0)\boldsymbol{A}(x_0^+). \tag{5.3}$$

At this point, the stress and displacement fields are known (from $\boldsymbol{A}(x)$ and $\boldsymbol{B}(x)$ and equation (2.6)) for $x_0 \leqslant x \leqslant x_1^+$. The procedure has to be iterated in the same manner until the waveguide outlet is reached.

6. Energy flux of reflected and transmitted waves

We start from the expression of the energy flux given in Appendix E (equation (E 7)),

$$\mathit{\Pi} = -\tfrac{1}{4}\mathrm{i}\omega(\boldsymbol{A}^{\mathrm{T}}\boldsymbol{J}^m\bar{\boldsymbol{A}} - \boldsymbol{B}^{\mathrm{T}}\boldsymbol{J}^m\bar{\boldsymbol{B}} - \boldsymbol{B}^{\mathrm{T}}\boldsymbol{J}^p\bar{\boldsymbol{A}} + \boldsymbol{A}^{\mathrm{T}}\boldsymbol{J}^p\bar{\boldsymbol{B}}), \tag{6.1}$$

where $\boldsymbol{J}^p$ and $\boldsymbol{J}^m$ are matrices defined in (E 8).

At the waveguide inlet, if the incident wave $\boldsymbol{A}(x_0^+)$ does not contain evanescent modes (for instance, by sending a right-going wave from infinity), the energy flux is reduced to

$$\mathit{\Pi}(x_0^+) = -\tfrac{1}{4}\mathrm{i}\omega\boldsymbol{A}^{\mathrm{T}}(x_0^+)J^m(x_0^+)\bar{\boldsymbol{A}}(x_0^+) - \boldsymbol{B}^{\mathrm{T}}(x_0^+)J^m(x_0^+)\bar{\boldsymbol{B}}(x_0^+)$$

(see Appendix E).

At the waveguide outlet, there is no leftward wave ($\boldsymbol{B}(x_N^-) = \boldsymbol{0}$) and the energy flux $\mathit{\Pi}(x_N^-)$ is reduced to

$$\mathit{\Pi}(x_N^-) = -\tfrac{1}{4}\mathrm{i}\omega(\boldsymbol{A}^{\mathrm{T}}(x_N^-)J^m(x_N^-)\bar{\boldsymbol{A}}(x_N^-)).$$

The energy flux conservation between the waveguide inlet and outlet leads to the equality $\mathit{\Pi}(x_0^+) = \mathit{\Pi}(x_N^-)$, and thus

$$\sum_n J_n(x_0^+)|A_n(x_0^+)|^2 = \sum_n J_n(x_0^+)|B_n(x_0^+)|^2 + \sum_n J_n(x_N^-)|A_n(x_N^-)|^2, \tag{6.2}$$

where the sum is performed on the propagating modes. Consequently, the fraction of energy flux of each propagating mode numbered by n, for an incident wave containing mode 0 only, is given by

$$\left.\begin{aligned} F_n^{\mathrm{r}} &= \frac{J_n(x_0^+)|B_n(x_0^+)|^2}{J_0(x_0^+)|A_0(x_0^+)|^2} \quad \text{in reflection,} \\ F_n^{\mathrm{t}} &= \frac{J_n(x_N^-)|A_n(x_N^-)|^2}{J_0(x_0^+)|A_0(x_0^+)|^2} \quad \text{in transmission.} \end{aligned}\right\} \tag{6.3}$$

Note that only propagating modes contribute to the energy flux at the extremities of the scattering region because evanescent modes cannot transport energy to infinity.

7. Results

In this section, we apply the method developed in the paper in three situations. For the sake of simplicity, only symmetric Lamb modes are considered, but a similar procedure can be performed for antisymmetric modes.

(*a*) *Validation*

The method presented is validated in the case of a bimaterial plate studied in Scandrett & Vasudevan (1991) for an aluminium/copper succession. The properties of the materials are given by the density ρ, the velocity of the free longitudinal wave $c_{\mathrm{l}} = ((\lambda+2\mu)/\rho)^{1/2}$ and the velocity of the free transverse wave $c_{\mathrm{t}} = (\mu/\rho)^{1/2}$. In the following, these properties have been taken to be the same as in the paper by Scandrett & Vasudevan (1991): $\rho = 2500\,\mathrm{kg\,m^{-3}}$, $c_{\mathrm{t}} = 3100\,\mathrm{m\,s^{-1}}$ and $c_{\mathrm{l}} = 6150\,\mathrm{m\,s^{-1}}$

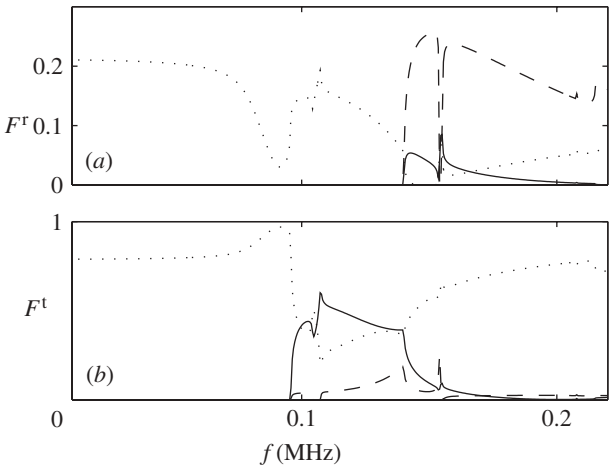

Figure 2. Fractions of energy flux reflected (a) and transmitted (b) as a function of frequency, for the three propagating modes, in the case of mode 0 incident from the left. The geometry is a bimaterial plate of semi-thickness $h = 1$ cm, aluminium to copper (properties of copper and aluminium are taken from Scandrett & Vasudevan (1991)): dotted line, mode 0; solid line, mode 1; dashed line, mode 2.

for aluminium; and $\rho = 3100\,\mathrm{kg\,m^{-3}}$, $c_\mathrm{t} = 2150\,\mathrm{m\,s^{-1}}$ and $c_\mathrm{l} = 4170\,\mathrm{m\,s^{-1}}$ for copper. Figure 2 shows in this case the fractions of energy flux reflected and transmitted for the three propagating modes (equation (6.3) with $n = 0, 1, 2$), with mode 0 incident from the left. The number of modes used to perform the calculations was 19. The results are quantitively in agreement with the results of Scandrett & Vasudevan (1991), except for a factor of *ca.* 2 on the frequency definition.

(b) *Results for a thick bonding*

We consider here a bimaterial plate corresponding to a thick bonding; it is a succession medium (1)–medium (2)–medium (1). Medium (1) is made of aluminium and medium (2) is made of copper. The source (mode 0 incident from the left) is placed at $x = x_0$ in medium (1). Between $x_1 > x_0$ and x_2, the plate is made of another medium (2); for $x \geqslant x_2$, the plate is again made of material (1), and the radiation condition at the right of the guide corresponds to no left-going waves only ($Z = I$). We have used equations (5.2) and (5.3) to calculate the whole displacement fields between x_0 and x_3 in a joint of copper in an aluminium plate of $h = 1$ cm semi-thickness; along the plate, $x_0 = 0$, $x_1 = 2$, $x_2 = 3$ and $x_3 = 5$ cm. Results are shown in figure 3 for different values of N_1 and N_2, numbers of considered modes, respectively, in aluminium (1) and in copper (2) at frequency $f = 1$ MHz. At this frequency, there is one propagating mode in aluminium and three in copper. For parts (a) and (b) of figure 3, the calculation has been performed while considering only the propagating modes in both media ($N_1 = 1$ and $N_2 = 3$). For parts (c) and (d), evanescent modes are included in the calculation ($N_1 = N_2 = 5$), and for parts (e) and (f), $N_1 = N_2 = 19$ has been used. It can be noticed that the fields obtained with a modest number of evanescent modes ($N_1 = N_2 = 5$) is already satisfying. Thus the multi-modal technique may be used by taking into account a reasonable number of evanescent modes.

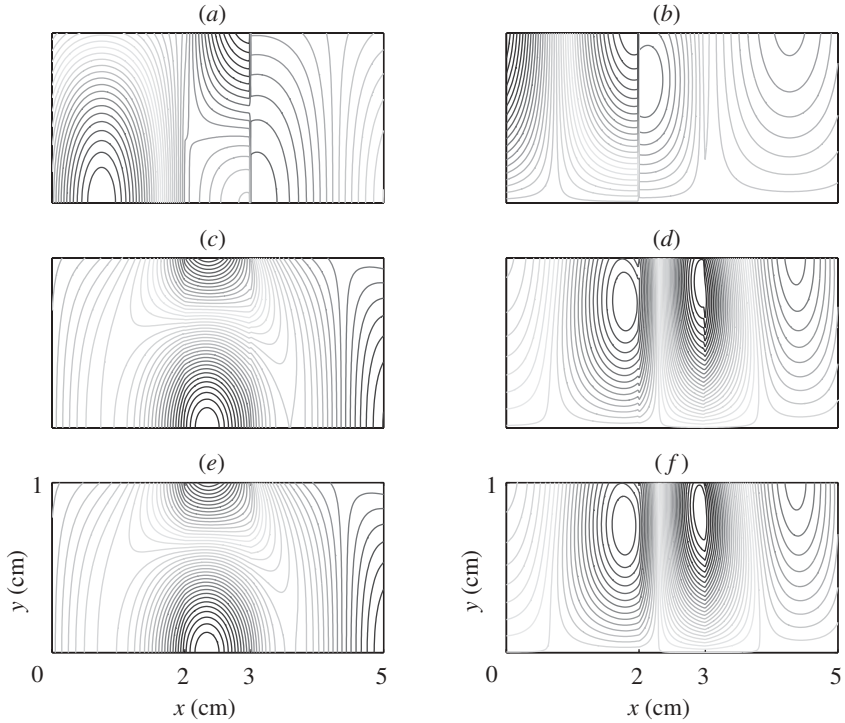

Figure 3. Displacement fields in a thick bonding of copper in a 1 cm semi-thickness plate of aluminium at frequency $f = 0.1$ MHz, with mode 0 incident from the left. The fields are calculated between 0 and 5 cm and the joint takes place between 2 and 3 cm. N_1 for aluminium and N_2 for copper are the numbers of modes considered in the calculation. (*a*) u and (*b*) v correspond to $N_1 = 1$ and $N_2 = 3$ (i.e. only propagating modes are considered). (*c*) u and (*d*) v correspond to $N_1 = N_2 = 5$. (*e*) u and (*f*) v correspond to $N_1 = N_2 = 19$.

Figure 4 shows the transmission F_n^{t} and reflection F_n^{r} coefficients (from equation (6.3) with $n = 0, 1, 2$) varying as functions of the frequency in a range such that mode 0 ($n = 0$), and then modes 1 and 2 ($n = 1$ and $n = 2$), become propagating. The source is again mode 0 incident from the left. For very low frequencies, the transmission coefficient tends to 1, which means that medium (2) is a small flaw that cannot be detected by a Lamb wave with a too-large wavelength. It can also be noticed that, for a frequency of *ca.* 0.1 MHz, the transmission coefficient of mode 0 reaches the value of 1, indicating a resonance in medium (2). Finally, when the frequency increases, multiple scattering effects produce more and more complicated behaviour of the reflection and transmission coefficients, when compared with the results of figure 2.

has?

(*c*) *Results for a periodic medium*

We consider here a plate of 1 cm semi-thickness made of a succession of N_p cells, each cell being composed of a slice of aluminium of length L and a slice of copper of length L. Calculations have been performed with N_1 modes in the aluminium medium and N_2 modes in the copper medium ($N_1 = N_2 = 19$). In all cases, mode 0 is incident from the left. Figure 5 shows the transmission coefficient of mode 0 as a

Author: what does subscript p denote?

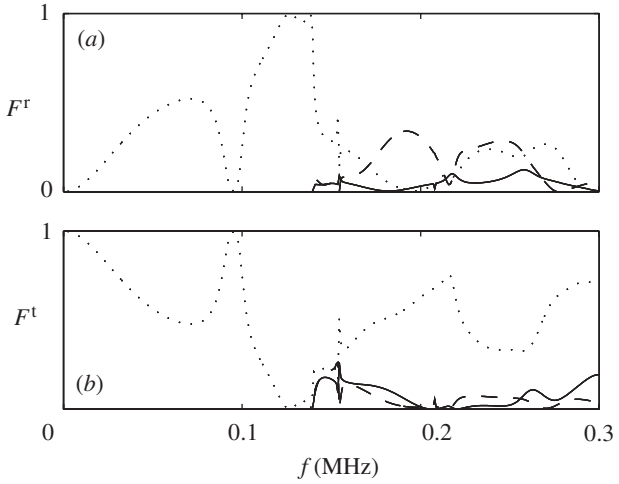

Figure 4. Fractions of energy flux reflected (a) and transmitted (b) for the three propagating modes, in the case of mode 0 incident from the left. The geometry is a thick bonding aluminium/copper/aluminium, as in figure 3: dotted line, mode 0; solid line, mode 1; dashed line, mode 2. Calculations are performed with $N_1 = N_2 = 19$, defined in figure 3.

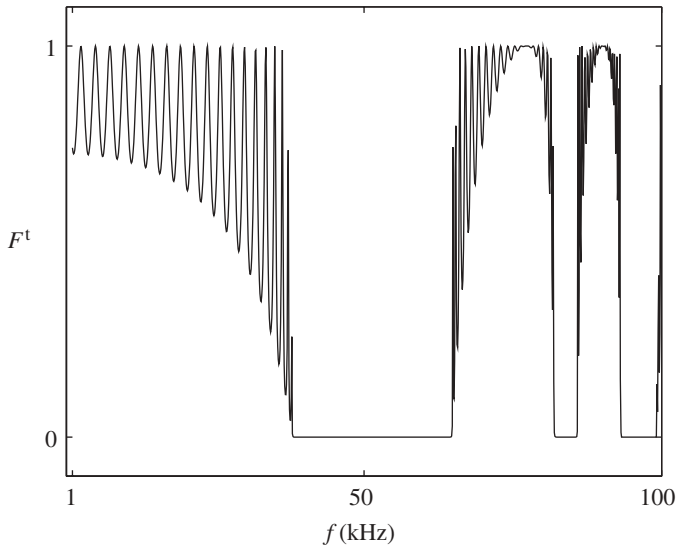

Figure 5. Transmitted energy flux ratio of the first propagating mode, in the case of mode 0 incident from the left, for a succession of $N_p = 20$ aluminium/copper cells in a 1 cm semi-thickness plate. The length of each medium is equal to $L = 2$ cm. Calculations are performed with $N_1 = N_2 = 19$, defined in figure 3.

function of the frequency in a range where only mode 0 is propagating. The length of each medium is equal to $L = 2$ cm, and the number of cells is $N_p = 20$. Figure 6 shows the transmission coefficient for $L = 5$ cm; in this latter case, part (a) corresponds to $N_p = 20$ and part (b) to $N_p = 50$. As expected in a periodic medium, stop-bands of zero transmission appear at frequencies whose values are roughly selected by a Bragg diffraction law type $k_{\mathrm{e}}L = n\pi$, with $k_{\mathrm{e}} = \frac{1}{2}(k_{\mathrm{a}} + k_{\mathrm{c}})$, where k_{a} (respectively, k_{c}) is

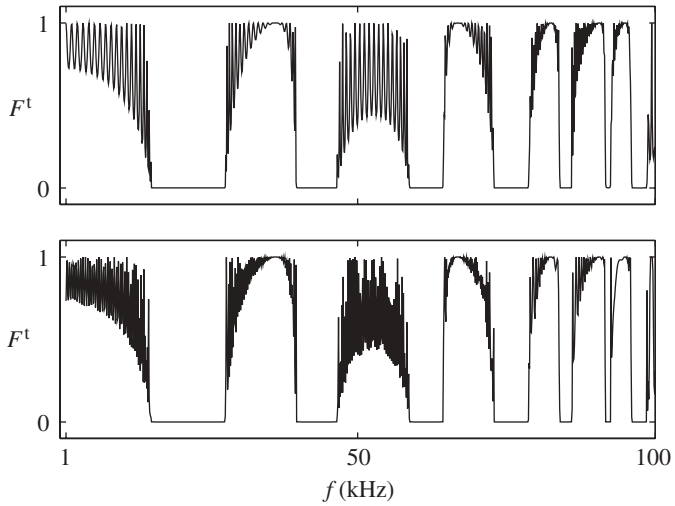

Figure 6. Transmitted energy flux ratio of the first propagating mode, in the case of mode 0 incident from the left, for a succession of (*a*) $N_p = 20$ and (*b*) $N_p = 50$ aluminium/copper cells in a 1 cm semi-thickness plate. Calculations are performed with the length of each medium equal to $L = 5$ cm and $N_1 = N_2 = 19$, defined in figure 3.

the wavenumber of mode 0 in aluminium (respectively, copper). Besides, oscillations in the pass-band are typical of the finite nature of the periodic medium. The oscillation number is related to the poles of the transmission coefficient in the complex plane. This number seems to be equal to $N_p - 1$, as it should be for one-dimensional propagation. As shown by Leng & Lent (1994), this property would be certainly lost for more than one propagating mode.

8. Closing remarks

A simple formalism has been developed to tackle the problem of Lamb wave propagation in axially layered plates. Owing to the introduction of the impedance matrix, this formalism permits the treatment of any multi-layered waveguide, with no limit on the number of modes that are taken into account. In the case where one is interested in the scattering properties of some part of waveguide, the computation of the impedance matrix, and thereafter of the reflection and transmission matrices, is sufficient and there is no need to compute the fields everywhere in the geometry.

The presented method can be easily extended to the study of other inhomogeneous plate involving the continuity of both displacements and horizontal stress forces. This is the case, for instance, of continuously axially layered waveguides, where the method could be applied, either by using the same equation as in this paper, with more and more thin slices of homogeneous waveguide, or by directly using a ordinary differential equation obtained by projecting the elasticity equation owing to equation (2.9). Work is under progress to apply this formalism to varying cross-section waveguides.

Appendix A. Dispersion relation and Lamb modes

The dispersion relation for symmetric modes is of the form (Viktorov 1967)

$$\frac{(\alpha_n^2+k_n^2)^2}{\alpha_n}\sinh(\alpha_n h)\cosh(\beta_n h)-4k_n^2\beta_n\sinh(\beta_n h)\cosh(\alpha_n h)=0, \tag{A 1}$$

with

$$\alpha_n=(k_n^2-k_{\mathrm{t}}^2)^{1/2}, \qquad \beta_n=(k_n^2-k_{\mathrm{l}}^2)^{1/2}$$

and

$$k_{\mathrm{t}}=\frac{\omega}{c_{\mathrm{t}}}=\left(\frac{\rho}{\mu}\right)^{1/2}\omega, \qquad k_{\mathrm{l}}=\frac{\omega}{c_{\mathrm{l}}}=\left(\frac{\rho}{\lambda+2\mu}\right)^{1/2}\omega.$$

The displacement and the stress vectors of symmetric Lamb modes can be written as a function of scalar potential ϕ_n and potential vector $(0,0,\psi_n)$, defined by

$$\left.\begin{aligned}\phi_n(x,y)&=(k_n^2+\alpha_n^2)\cosh(\beta_n y)\sinh(\alpha_n h),\\ \psi_n(x,y)&=-2\mathrm{i}k_n\beta_n\sinh(\alpha_n y)\sinh(\beta_n h),\end{aligned}\right\} \tag{A 2}$$

with

$$\begin{aligned}U_n&=\mathrm{i}k_n\phi_n+\partial_y\psi_n\\ &=\mathrm{i}k_n(k_n^2+\alpha_n^2)\cosh(\beta_n y)\sinh(\alpha_n h)-2\mathrm{i}k_n\beta_n\alpha_n\cosh(\alpha_n y)\sinh(\beta_n h), &\text{(A 3)}\\ V_n&=\partial_y\phi_n-\mathrm{i}k_n\psi_n\\ &=\beta_n(k_n^2+\alpha_n^2)\sinh(\beta_n y)\sinh(\alpha_n h)-2\beta_n k_n^2\sinh(\alpha_n y)\sinh(\beta_n h), &\text{(A 4)}\\ S_n&=\mu[-(k_n^2+2\beta_n^2-\alpha_n^2)\phi_n+2\mathrm{i}k_n\partial_y\psi_n]\\ &=\mu[(-2\beta_n^2+\alpha_n^2-k_n^2)(k_n^2+\alpha_n^2)\cosh(\beta_n y)\sinh(\alpha_n h)\\ &\qquad\qquad+4k_n^2\beta_n\alpha_n\cosh(\alpha_n y)\sinh(\beta_n h)], &\text{(A 5)}\\ T_n&=\mu[2\mathrm{i}k_n\partial_y\phi_n+(k_n^2+\alpha_n^2)\psi_n]\\ &=\mu 2\mathrm{i}k_n\beta_n(k_n^2+\alpha_n^2)[-\sinh(\alpha_n y)\sinh(\beta_n h)+\sinh(\beta_n y)\sinh(\alpha_n h)]. &\text{(A 6)}\end{aligned}$$

Appendix B. Biorthogonality relation and expression of J_n

The biorthogonality condition (Fraser 1976) for an in-plane problem can be written

$$(X_n\mid Y_m)=\int_{-h}^{h}(-U_nS_m+V_mT_n)\,\mathrm{d}y=J_n\delta_{nm}. \tag{B 1}$$

J_n can be conveniently expressed using ϕ_n and ψ_n,

$$\begin{aligned}(X_n\mid Y_n)=\mu\int_{-h}^{h}[\mathrm{i}k_n(\alpha_n^2-k_n^2)(\phi_n^2-\psi_n^2)+2(\alpha_n^2-\beta_n^2)\phi_n\psi_n]\,\mathrm{d}y\\ -\mu[2\mathrm{i}k_n(\phi_n\phi_n'-\psi_n\psi_n')-(\alpha_n^2+3k_n^2)\phi_n\psi_n]_{-h}^{h}.\end{aligned} \tag{B 2}$$

For symmetric modes, J_n is given by

$$J_n = \mu \mathrm{i} k_n (k_n^2 - \alpha_n^2) \times \left\{ \sinh^2(\alpha_n h) \sinh^2(\beta_n h) \left[\frac{(k_n^2 + \alpha_n^2)(k_n^2 + \alpha_n^2 - 8\beta_n^2)}{\beta_n \tanh(\beta_n h)} + \frac{4\beta_n^2 (k_n^2 + 2\alpha_n^2)}{\alpha_n \tanh(\alpha_n h)} \right] + h[-4k_n^2 \beta_n^2 \sinh^2(\beta_n h) + (k_n^2 + \alpha_n^2)^2 \sinh^2(\alpha_n h)] \right\}. \tag{B 3}$$

Appendix C. Calculation of the impedance matrix in a single medium

Starting from (3.3), it is straightforward to find

$$\boldsymbol{Z}(x') = [\mathrm{i}\boldsymbol{S}(x' - x) + \boldsymbol{C}(x' - x)\boldsymbol{Z}(x)][\boldsymbol{C}(x' - x) + \mathrm{i}\boldsymbol{S}(x' - x)\boldsymbol{Z}(x)]^{-1}. \tag{C 1}$$

Application of this equation to a real case causes a divergence resembling the divergence of a stiff differential equation. This is because the elements of the matrices $\boldsymbol{C}$ and $\boldsymbol{S}$ contain very large numbers for the evanescent modes, which cause exponential divergence of the computation due to the finite numerical precision. Another form (3.4) can be found in the following way:

$$\begin{aligned} \boldsymbol{Z}(x') &= -\mathrm{i}\{\mathrm{i}\boldsymbol{S}^{-1}(x' - x) + \boldsymbol{C}(x' - x)[\boldsymbol{Z}(x) - \mathrm{i}\boldsymbol{H}^{-1}(x' - x)]\} \\ &\qquad \times [\boldsymbol{Z}(x) - \mathrm{i}\boldsymbol{H}^{-1}(x' - x)]^{-1} \boldsymbol{S}^{-1}(x' - x) \\ &= -\mathrm{i}\boldsymbol{H}^{-1}(x' - x) + \boldsymbol{S}^{-1}(x' - x)[\boldsymbol{Z}(x) - \mathrm{i}\boldsymbol{H}^{-1}(x' - x)]^{-1} \boldsymbol{S}^{-1}(x' - x). \end{aligned} \tag{C 2}$$

Some resonance can occur for discrete values of $(x' - x)$ when the denominators are going to zero, but, in practice, it did not appear that a special numerical care has to be taken to avoid it.

Another issue is now the sign of $(x' - x)$ when using this equation. If we denote by $\boldsymbol{M}$ the matrix $\underline{[\boldsymbol{Z}(x) - \mathrm{i}\boldsymbol{H}^{-1}(x' - x)]^{-1}}$, equation (C 2) implies that

Extra '(' removed – OK?

$$Z_{mn}(x') = -\mathrm{i}[\tan k_n(x' - x)]^{-1} \delta_{mn} + [\sin k_m(x' - x) \sin k_n(x' - x)]^{-1} M_{mn}.$$

In the right-hand side, and unless k_n and k_m are real numbers, the first term tends towards ± 1 when $(x' - x)$ tends towards $\mp\infty$ and the second term tends towards zero. Thus we have

$$\boldsymbol{Z}(x') \xrightarrow{(x'-x)\to\pm\infty} \begin{pmatrix} \boldsymbol{Z}_\mathrm{p} & 0 \\ 0 & \mp\boldsymbol{I} \end{pmatrix}, \tag{C 3}$$

where $\boldsymbol{Z}_\mathrm{p}$ refers to the impedance restricted to propagating modes, i.e. the modes with real wavenumbers.

All this means that equation (C 2) must be used in the direction that has physical sense. If we impose a radiation condition of anechoic termination towards the right-hand side of x by imposing a numerical initial condition $\boldsymbol{Z}(x) = \boldsymbol{I}$, equation (C 2) can be used towards the left-hand side of x where $\boldsymbol{I}$ is invariant, but equation (C 2) cannot be used towards the right-hand side of x where $\boldsymbol{I}$ will not be invariant.

Appendix D. Expression of matrices F and G

F and G are given by

$$G_{mn} = (J_n^+)^{-1}(X_n^- \mid Y_m^+), \tag{D 1}$$

$$F_{mn} = (J_n^-)^{-1}(X_m^- \mid Y_n^+). \tag{D 2}$$

Calculating $(X_n^- \mid Y_m^+)$ allows us to calculate both F and G. For the sake of clarity, in the following expression, index m refers to quantities calculated using k_m^+ and n to quantities calculated using k_n^-. With $L_\mu = \mu^+/\mu^-$, we have

$$\begin{aligned}
&\frac{1}{\mu^+}(X_n \mid Y_m) \\
&\quad = 2\mathrm{i}\frac{\sinh(\alpha_m h)\sinh(\beta_m h)}{\sinh(\alpha_n h)\sinh(\beta_n h)} \\
&\qquad \times \Bigg\{ 2\alpha_n k_n (k_n^2+\alpha_n^2)(k_m^2+\alpha_m^2)\left(\frac{\beta_m}{\tanh(\beta_n h)} - \frac{\beta_n}{\tanh(\beta_m h)}\right) \\
&\qquad\quad + \frac{k_n(k_m^2 + 2\beta_m^2 - \alpha_m^2 - 2L_\mu\beta_m^2)(k_n^2+\alpha_n^2)(k_m^2+\alpha_m^2)}{\beta_n^2-\beta_m^2} \\
&\qquad\qquad\qquad \times \left(\frac{\beta_n}{\tanh(\beta_m h)} - \frac{\beta_m}{\tanh(\beta_n h)}\right) \\
&\qquad\quad - 2\frac{k_n\beta_n\alpha_n[k_m^2 + 2\beta_m^2 - \alpha_m^2 - L_\mu(k_n^2+\alpha_n^2)](k_m^2+\alpha_m^2)}{\alpha_n^2-\beta_m^2} \\
&\qquad\qquad\qquad \times \left(\frac{\alpha_n}{\tanh(\beta_m h)} - \frac{\beta_m}{\tanh(\alpha_n h)}\right) \\
&\qquad\quad + 4(1-L_\mu)\frac{k_n k_m^2 \beta_n\beta_m(k_n^2+\alpha_n^2)}{\alpha_m^2-\beta_n^2}\left(\frac{\alpha_m}{\tanh(\alpha_m h)} - \frac{\beta_n}{\tanh(\beta_n h)}\right) \\
&\qquad\quad - 4k_n k_m^2\beta_m\left(\frac{k_n^2+\alpha_n^2}{\tanh(\beta_n h)} - \frac{2\beta_n\alpha_n}{\tanh(\alpha_n h)}\right) \\
&\qquad\quad - 4\frac{k_n k_m^2\beta_n\beta_m[2\alpha_n^2 - L_\mu(k_n^2+\alpha_n^2)]}{\alpha_n^2-\alpha_m^2}\left(\frac{\alpha_n}{\tanh(\alpha_n h)} - \frac{\alpha_m}{\tanh(\alpha_m h)}\right)\Bigg\}.
\end{aligned} \tag{D 3}$$

Appendix E. Derivation of the energy flux

In this section, we denote by X_i the real instantaneous value of X, and by $\dot{X}$ and $\ddot{X}$, respectively, the first and second time derivative of X. We start from the elasticity equation, written in the temporal domain as $\rho\ddot{\boldsymbol{w}}_i = \operatorname{div}\sigma_i$. Taking the scalar product of this equation with $\dot{\boldsymbol{w}}_i$ and using $\operatorname{div}(\sigma_i\dot{\boldsymbol{w}}_i) = (\operatorname{div}\sigma_i)\dot{\boldsymbol{w}}_i + (\sigma_i : \nabla\dot{\boldsymbol{w}}_i)$, we obtain $\partial_t(\frac{1}{2}\rho\dot{\boldsymbol{w}}_i^2) + (\sigma_i : \nabla\dot{\boldsymbol{w}}_i) = \operatorname{div}(\sigma_i\dot{\boldsymbol{w}}_i)$.

We now introduce the tensor of deformation ϵ_i, defined by $\epsilon_i = \frac{1}{2}(\nabla\boldsymbol{w}_i + (\nabla\boldsymbol{w}_i)^{\mathrm{T}})$; σ_i is related to ϵ_i by $\sigma_i = \lambda\,\mathrm{tr}(\epsilon_i)\mathrm{I} + 2\mu\epsilon_i$. With the tensorial product of symmetric and antisymmetric tensors being equal to zero, we have $(\sigma_i : \nabla\dot{\boldsymbol{w}}_i) = (\sigma_i : \dot{\epsilon}_i)$. Consequently, $(\sigma_i : \nabla\dot{\boldsymbol{w}}_i) = \lambda\,\mathrm{tr}(\epsilon_i)(\mathrm{I} : \dot{\epsilon}_i) + 2\mu(\epsilon_i : \dot{\epsilon}_i)$. With $(\mathrm{I} : \dot{\epsilon}_i) = \mathrm{tr}(\dot{\epsilon}_i)$, we have $(\sigma_i : \nabla\dot{\boldsymbol{w}}_i) = \partial_t(\frac{1}{2}\lambda\,\mathrm{tr}(\epsilon_i^2) + \mu(\epsilon_i : \epsilon_i))$. Finally, the equation of energy conservation is

Author: transpose T in correct position?

derived as

$$\partial_t e_i + \operatorname{div} \boldsymbol{\pi}_i = 0, \tag{E 1}$$

with e_i the total energy,

$$e_i = \tfrac{1}{2}\rho \dot{\boldsymbol{w}}_i^2 + \tfrac{1}{2}\lambda \operatorname{tr}(\epsilon_i^2) + \mu(\epsilon_i : \epsilon_i), \tag{E 2}$$

and $\boldsymbol{\pi}_i$ the energy flux vector,

$$\boldsymbol{\pi}_i = -\sigma_i \dot{\boldsymbol{w}}_i. \tag{E 3}$$

In a waveguide, the time-averaged total energy flux across a section

$$\mathit{\Pi} = \int_S \langle \boldsymbol{\pi}_i \rangle \, \mathrm{d}\boldsymbol{S}$$

at a given frequency ω can be conveniently expressed as a function of $\boldsymbol{a}$ and $\boldsymbol{b}$. We have, in this case, $\langle \boldsymbol{\pi}_i \rangle = -\frac{1}{4}\mathrm{i}\omega(\sigma\bar{\boldsymbol{w}} - \bar{\sigma}\boldsymbol{w})$, leading to

$$\mathit{\Pi} = -\tfrac{1}{4}\mathrm{i}\omega \int_S (s\bar{u} + t\bar{v} - \bar{s}u - \bar{t}v). \tag{E 4}$$

The fact that equation (E 4) resembles a linear combination of the biorthogonality conditions comes from the kind of similarities shared by the biorthogonality and the energy conservation. On the one hand, the biorthogonality is, in part, derived owing to the reciprocity relation (Murphy & Li 1994). On the other hand, the conservation of energy flux can be viewed as being derived from the reciprocity relation between the field solution and its conjugate, the latter also being a solution because of the time reversal symmetry.

With $u = \boldsymbol{a}^{\mathrm{T}}\boldsymbol{U}$, $v = \boldsymbol{b}^{\mathrm{T}}\boldsymbol{V}$, $s = \boldsymbol{b}^{\mathrm{T}}\boldsymbol{S}$ and $t = \boldsymbol{a}^{\mathrm{T}}\boldsymbol{T}$, $\mathit{\Pi}$ takes the form

$$\mathit{\Pi} = -\tfrac{1}{4}\mathrm{i}\omega(\boldsymbol{a}^{\mathrm{T}}\mathit{J}\bar{\boldsymbol{b}} - \boldsymbol{b}^{\mathrm{T}}\bar{\mathit{J}}^{\mathrm{T}}\bar{\boldsymbol{a}}), \tag{E 5}$$

where $\mathit{J}_{mn} = (X_m \mid \bar{Y}_n)$. A typical example of the J matrix structure is given here in a particular (but representative) case. We consider two propagating modes (k_0 and k_1 real, leading to J_0 and J_1 purely imaginary) and three evanescent modes, two of them associated with k_2 and its complex conjugate $k_3 = \bar{k}_2$ (leading to $J_3 = \bar{J}_2$), and one associated with a purely imaginary wavenumber k_4 (leading to J_4 real). J takes the form

$$\mathit{J} = \begin{pmatrix} J_0 & 0 & 0 & 0 & 0 \\ 0 & J_1 & 0 & 0 & 0 \\ 0 & 0 & 0 & J_2 & 0 \\ 0 & 0 & \bar{J}_2 & 0 & 0 \\ 0 & 0 & 0 & 0 & J_4 \end{pmatrix}. \tag{E 6}$$

Finally, $\mathit{\Pi}$ can be expressed as a function of the right- and left-going waves using $\boldsymbol{a} = \boldsymbol{A} - \boldsymbol{B}$ and $\boldsymbol{b} = \boldsymbol{A} + \boldsymbol{B}$,

$$\mathit{\Pi} = -\tfrac{1}{4}\mathrm{i}\omega(\boldsymbol{A}^{\mathrm{T}}\mathit{J}^m\bar{\boldsymbol{A}} - \boldsymbol{B}^{\mathrm{T}}\mathit{J}^m\bar{\boldsymbol{B}} - \boldsymbol{B}^{\mathrm{T}}\mathit{J}^p\bar{\boldsymbol{A}} + \boldsymbol{A}^{\mathrm{T}}\mathit{J}^p\bar{\boldsymbol{B}}), \tag{E 7}$$

with $\mathit{J}^p = \mathit{J} + \bar{\mathit{J}}^{\mathrm{T}}$ and $\mathit{J}^m = \mathit{J} - \bar{\mathit{J}}^{\mathrm{T}}$. The structures of the J^m and J^p matrices are given in the previous example,

$$\mathit{J}^m = 2\begin{pmatrix} J_0 & 0 & 0 & 0 & 0 \\ 0 & J_1 & 0 & 0 & 0 \\ 0 & 0 & 0 & 0 & 0 \\ 0 & 0 & 0 & 0 & 0 \\ 0 & 0 & 0 & 0 & 0 \end{pmatrix} \quad \text{and} \quad \mathit{J}^p = 2\begin{pmatrix} 0 & 0 & 0 & 0 & 0 \\ 0 & 0 & 0 & 0 & 0 \\ 0 & 0 & 0 & J_2 & 0 \\ 0 & 0 & \bar{J}_2 & 0 & 0 \\ 0 & 0 & 0 & 0 & J_4 \end{pmatrix}. \tag{E 8}$$

As a consequence, if the incoming wave $\boldsymbol{A}$ at a given position x does not contain evanescent modes, the energy flux $\mathit{\Pi}$ at x takes the simplest form,

$$\mathit{\Pi} = -\tfrac{1}{4}\mathrm{i}\omega(\boldsymbol{A}^{\mathrm{T}} J^m \bar{\boldsymbol{A}} - \boldsymbol{B}^{\mathrm{T}} J^m \bar{\boldsymbol{B}}),$$

in which case it can be seen that only propagating modes contribute to the energy flux. For more general cases, if $\boldsymbol{A}$ and $\boldsymbol{B}$ contain evanescent modes, then some energy can be transported by the evanescent modes (Auld 1973).

References

Achenbach, J. D. 1987 *Wave propagation in elastic solids*. Amsterdam: North-Holland.

Auld, B. A. 1973 *Acoustic fields and waves in solids*, vol. II. Wiley.

Folguera, A. & Harris, G. H. 1999 Coupled Rayleigh surface in a slowly varying elastic waveguide. *Proc. R. Soc. Lond.* A **455**, 917–931.

Fraser, W. B. 1976 Orthogonality relation for the Rayleigh–Lamb modes of vibration of a plate. *J. Acoust. Soc. Am.* **59**, 215–216.

Galanenko, V. B. 1998 On coupled modes theory of two-dimensional wave motion in elastic waveguides with slowly varying parameters in curvilinear orthogonal coordinates. *J. Acoust. Soc. Am.* **103**, 1752–1762.

Givoli, D. 1992 *Numerical methods for problems in infinite domains*. Elsevier.

Gregory, R. D. & Gladwell, I. 1983 The reflection of a symmetric Rayleigh–Lamb wave at a fixed or free edge of a plate. *J. Elastic.* **13**, 185–206.

Kirrmann, P. 1995 On the completeness of Lamb modes. *J. Elastic.* **37**, 39–69.

Leng, M. & Lent, C. S. 1994 Conductance quantization in a periodically modulated channel. *Phys. Rev.* B **50**, 10 823–10 833.

Miklowitz, J. 1978 *The theory of elastic waves and waveguides*, ch. 4. Amsterdam: North-Holland.

Morse, P. & Ingard, U. 1952 *Theoretical acoustics*. McGraw-Hill.

Murphy, J. E. & Li, G. 1994 Orthogonality relation for Rayleigh–Lamb modes of vibration of an arbitrarily layered elastic plate with and without fluid loading. *J. Acoust. Soc. Am.* **96**, 2313–2317.

Pagneux, V. & Maurel, A. 2001 Determination of Lamb mode eigenvalues. *J. Acoust. Soc. Am.* **110**. (In the press.). Details?

Pagneux, V., Amir, N. & Kergomard, J. 1996 A study of wave propagation in varying cross-section waveguides by modal decomposition. Part I. Theory and validation. *J. Acoust. Soc. Am.* **100**, 2034–2048.

Predoi, M. V. & Rousseau, M. 2000 Réflexion et transmission d'un mode de Lamb au niveau d'une soudure entre deux plaques. In *Proc. 5th French Congress on Acoustics*, pp. 173–176. Presses Polytechniques et Universitaires Romandes.

Scandrett, C. & Vasudevan, N. 1991 The propagation of time harmonic Rayleigh–Lamb waves in a bimaterial plate. *J. Acoust. Soc. Am.* **89**, 1606–1614.

Viktorov, I. A. 1967 *Rayleigh and Lamb waves: physical theory and applications*, ch. 2. New York: Plenum.